www.project-foci.eu

Co-funded by the European Union

UK Research and Innovation

Horizon Europe

(HORIZON-CL5-2021-D1-01)

Non-CO2 Forcers and their Climate, Weather, Air Quality and Health Impacts

FOCI

Deliverable 3.3

Model improvements on aerosol-cloud interactions

Grant agreement No 101056783

Grant Agreement No.	101056783	
Project acronym	FOCI	
Project full title	Non-CO2 Forcers and their Climate, Weather, Air Quality and Health Impacts	
Call	HORIZON-CL5-2021-D1-01	
Deliverable name	D3.3 Model improvements on aerosol-cloud interactions	
WP contributing to the deliverable	WP3	
Task producing the deliverable	Task 3.3 Aerosol-cloud interactions	
Type	x	Report
		Prototype
		Demonstrator
		Other: Data
Dissemination level	x	Public
		Sensitive
		UE/EU-Restricted
Due date of deliverable	Month 30	
Actual submission date	Month 36	
Lead beneficiary	BSC	
Author(s)	Twan van Noije (KNMI), Lianghai Wu (KNMI), Philippe Le Sager (KNMI), Vincent Huijnen (KNMI), Tommi Bergman (FMI), Harri Kokkola (FMI), Anton Laakso (FMI), María Gonçalves-Ageitos (BSC), Marios Chatziparaschos (BSC), Montserrat Costa Surós (BSC), Carlos Pérez García-Pando (BSC), Oriol Jorba (BSC), Sergey Gromov (MPI-C), Andrea Pozzer (MPI-C)	
Other Contributor(s)		
Reviewer(s)	Jonathan Wilkinson (ECMWF)	
Keywords	FOCI, deliverables, model improvements	

ACKNOWLEDGEMENTS

This project has been co-funded by the European Union with funding from the European Union's Horizon Europe research and innovation programme under grant agreement No. 101056783 and from UKRI under the UK Government's Horizon Europe Guarantee (UKRI Reference Numbers: 10040465, 10053814 and 10050799).

Version	Date	Modified by	Comments
0.0	10 Jun 2025	Oriol Jorba	First draft shared with co-authors
0.1	21 Aug 2025	Oriol Jorba and co-authors	Second draft version with input from co-authors shared with reviewer
1.0	26 Aug 2025	Oriol Jorba and co-authors	Complete version with input from co-authors and revision to incorporate reviewer's comments

	Name	Date
Verification Final Draft by WP leaders	Oriol Jorba (BSC), Twan van Noije (KNMI)	30 Aug 2025
Check before upload by project Coordinator	Tomas Halenka (CU)	31 Aug 2025

TABLE OF CONTENTS

EXECUTIVE SUMMARY

This document is the deliverable "D3.3: Model improvements on aerosol-cloud interactions" for the European Union project "FOCI: Non-CO2 Forcers and their Climate, Weather, Air Quality and Health Impacts" (hereinafter also referred to as FOCI, project reference: 101056783).

The report describes the model development and improvements of the representation of aerosol-cloud interactions in both EC-Earth4 and EMAC Earth System Models. In particular, for EC-Earth, aerosol activation was previously not represented in IFS and OpenIFS and has been implemented in OpenIFS 48r1 through the porting of the EC-Earth3 activation scheme based on Abdul-Razzak and Ghan (2000) and its coupling to radiation and cloud microphysics. This work was extended with the improved activation parameterization from Morales Betancourt and Nenes (2014) together with Gauss–Legendre quadrature for vertical velocity integration, a TKE-based parameterization of sub-grid vertical velocity variability, and the deep learning–based "Wnet" scheme (Barahona et al., 2023). Within FOCI, we supported these developments by testing the new activation code and merging it with other aerosol–chemistry modules described in Deliverable D3.1. Furthermore, work towards the integration of the effect of dust minerals, particularly quartz and k-feldspars, as efficient ice nucleators and their impact on mixed-phase clouds formation have also been conducted through the implementation of a new dust emission module in Open IFS based on Tegen et al. (2002, 2004) enabling the calculation of the mineral mass fraction at emission of quartz and k-feldspar, and their link to the ice crystal number concentration (ICNC) calculation in OpenIFS 48r1. For EMAC, the standard aerosol activation method based on Abdul-Razzak and Ghan (2000) scheme has been complemented with two additional activation parametrizations, the one from Barahona and Nenes (2009), specifically developed for ice and mixed phase clouds and the one of Morales Betancourt and Nenes (2014), specifically developed for warm clouds.

Some basic evaluations have been performed as part of the development cycle, and more detailed evaluations against a larger set of observational data sets will be performed within Task 3.4 of the work package (WP3). In this report we aim to document the new model developments.

CONTRIBUTION TO THE FOCI OBJECTIVES

This deliverable is the third of a series of reports on the Earth system model development activities in WP3. The work described in this report contributes to the project objective O4:

"To improve and evaluate state-of-the-art global ESMs (WP3) and regional climate and atmospheric composition models (RCMs) (WP4), targeting specific critical processes with the largest uncertainties (WP6) for improving future next generation climate projections."

Through this, it will contribute to the aims of WP8 under objective O7 to implement a global outreach on the overall improvement of chemistry-climate interaction in new CMIP7 cycle and up-to-date capability of the ESM to capture aerosols interaction in these processes.

1. INTRODUCTION

This report describes the developments introduced in the representation of key aerosol-cloud interaction processes associated with non-CO2 climate forcers in two ESMs, EC-Earth4 and EMAC. EC-Earth4 is the next version of the European consortium ESM EC-Earth, which is currently under development and being prepared for application in the Coupled Model Intercomparison Project phase 7 (CMIP7). The atmospheric general circulation model of EC-Earth4 is based on the OpenIFS model from the ECMWF. EMAC (ECHAM5/MESSy Atmospheric Chemistry) is a modular ESM developed through a multi-institutional effort. It employs the Modular Earth Submodel System (MESSy) framework to integrate various scientific codes, enabling detailed studies of atmospheric chemistry and its interactions with the climate system. Within both EC-Earth4 and EMAC, new aerosol activation parameterizations have been introduced and extensions towards the integration of dust minerals, particularly quartz and k-feldspars, as ice nucleators in mixed-phase clouds formation within EC-Earth4 have been implemented. Initial evaluations of these new implementations are briefly reported here. More extensive assessments against broader observational datasets are planned within Task 3.4 of WP3 and will be reported in Deliverable D3.4.

2. DESCRIPTION OF MODEL REVISIONS

2.1 EC-Earth4

Aerosol-cloud interactions in EC-Earth comprise of multiple processes. First, the formation of cloud droplets depends on the presence of aerosols that can act as cloud condensation nuclei. The activation of aerosols to initiate droplet formation depends on the maximum supersaturation in rising air parcels and hence on the vertical velocity at sub-grid scale level. The activation process determines the cloud droplet number concentration (CDNC) in newly formed clouds, which is combined with the cloud liquid water content to estimate the droplet effective radius that enters the radiative transfer calculation. Moreover, the CDNC calculated in the activation scheme also determines the rate of autoconversion and accretion in the cloud microphysics scheme. In mixed-phase clouds, the ice crystal number concentration (ICNC) is determined by ice nucleation possibly in combination with secondary ice production (SIP). The resulting ICNC is used as a basis to parametrize the depositional growth of ice crystals. Finally, aerosol-cloud interactions also include the scavenging of aerosols by precipitation formation in convective and stratiform clouds.

The description of these processes has evolved over the different versions of the model. In the CMIP6 configurations of EC-Earth (including EC-Earth3 and EC-Earth3-AerChem), aerosol activation is described following the parametrization from Abdul-Razzak and Ghan (2000), assuming that the sub-grid variations in vertical velocity follow a normal distribution with a fixed standard deviation, which is set to 0.8 m/s. The averaging over this distribution is performed by calling the activation at equidistant velocity values that sample the distribution, where the default number of discretization points is set to 10. For mixed-phase clouds, it is assumed that homogenous freezing occurs instantaneously at temperatures lower than -38ºC, while between -38ºC and 0ºC supercooled liquid water and ice can coexist. ICNC is diagnosed following the IFS cycle 36r4 implementation of the deposition-condensation-freezing nucleation parameterization of Meyers et al. (1992), which primarily depends on temperature.

The EC-Earth3-AerChem version used for the CMIP6 exercise has seen several updates with respect to both cloud droplet and ice crystal formation. Much of this work was carried out as part of the EU Horizon 2020 project FORCeS (Salvinen et al., submitted; Thomas et al., 2024). Regarding the activation of aerosols for droplet formation, an improved parameterization based on the population-splitting method of Morales Betancourt and Nenes (2014) was introduced. In addition, the integration over the updraft velocities has been

made more computationally efficient by introducing Gauss-Legendre quadrature, which allowed to reduce the number of quadrature points to 3. Concerning mixed-phase clouds, a combination of an aerosol-sensitive primary ice parameterization combined with a machine learning-based parameterization of secondary ice production (SIP) was introduced.

EC-Earth4, under development at present, constitutes the new generation of the EC-Earth model to contribute to CMIP7, and relies on a more recent IFS cycle, 48r1. Within FOCI, work has been devoted to bringing into EC-Earth4 some of the recent advances in the representation of aerosol-cloud interactions.

In deliverable "D3.1: Model improvements for physico-chemical processes of non-CO2 radiative forcers", we have reported on the development and integration of a new aerosol scheme in EC-Earth4 and have given an overview of the various improvements in the representation of physico-chemical processes of non-CO2 radiative forcers in EC-Earth4. The developments reported in D3.1 include an improved description of aerosol activation and aerosol wet scavenging. For details on the revisions in the description of scavenging, we refer to D3.1; in the next subsection we will provide more details on the improved description of activation and ice crystal formation.

2.1.1 Activation scheme

Aerosol activation is not explicitly represented in either the IFS or OpenIFS. As part of the integration of the new HAM based modal aerosol module in EC-Earth4, the EC-Earth3 code for calculating activation based on Abdul-Razzak and Ghan (2000) was ported to OpenIFS 43r3 and then to the new OpenIFS version, 48r1. The implementation of this scheme follows that in EC-Earth3, including the treatment of the updraft vertical velocity and the way CDNC is coupled to the radiation scheme and the cloud microphysics (van Noije et al., 2021). Next, the improved activation parameterization from Morales Betancourt and Nenes (2014) was introduced together with Gauss-Legendre quadrature to perform the vertical velocity integration. This code was ported from the EC-Earth3 FORCeS version into OpenIFS 48r1 as part of the Horizon Europe project CleanCloud. As part of that work, a parameterization of the sub-grid scale vertical velocity variability depending on turbulent kinetic energy (TKE) as well as a deep learning parameterization called "Wnet" from Barahona et al. (2023) have been introduced. Within FOCI, we have supported these developments by testing the new activation code and merging it with the other aerosol and chemistry related OpenIFS developments documented in D3.1. As part of this activity, we have also refactored the codebase of the new activation scheme from Fortran 77 to Fortran 99.

2.1.2 Effects of mineral dust on mixed-phase clouds

Dust minerals, particularly quartz and k-feldspars, act as efficient ice nucleators and can impact mixed-phase clouds formation (e.g., Harrison et al., 2019). The work conducted in FOCI towards the integration of these effects in EC-Earth4 follows different stages. First, the Tegen et al. (2002, 2004) dust emission module has been implemented in OpenIFS 48r1. Then, the mineral mass fraction at emission for quartz and k-feldspar has to be estimated. Finally, the abundance of ice nucleating particles has to be linked to the ice crystal number concentration (ICNC) in OpenIFS 48r1 to describe the primary ice production in mixed-phase clouds.

The background for the implementation of the Tegen et al. (2002, 2004) dust emission scheme has been described in Deliverable D3.1 of FOCI. The work consisted in the introduction in OpenIFS 48r1 of a set of boundary conditions (e.g., soil types, roughness length, dust preferential sources, etc.), their interpolation to the model grid and the introduction of the Tegen et al. (2002, 2004) dust scheme. Dust emission involves complex processes that are poorly understood, and many times occur at smaller scales than global Earth System Models can solve, therefore they are usually calibrated against observations. We aim at scaling the OpenIFS 48r1 new

dust emission flux globally (i.e., applying a constant factor) using a combination of observation-based evidence. First, the global average annual mean dust optical depth (DOD) at 550 nm must be close to the observationally constrained value of 0.03±0.01 (95% confidence interval) in present day climate conditions (Ryder et al., 2016; Voss and Evan, 2020; Gkikas et al., 2021). Then, the annual mean modelled surface dust concentration is compared to reference climatological data from the Rosenstiel School of Marine and Atmospheric Science (RSMAS) of the University of Miami (Arimoto et al., 1995; Prospero, 1996, 1999) and the African Aerosol Multidisciplinary Analysis (AMMA) (Marticorena et al., 2010), the annual mean modelled dust deposition flux is compared to a reference dataset compiled in Albani et al. (2014) and the dust optical depth at 550 nm, to a climatology of dust-filtered NASA AErosol RObotic NETwork (AERONET) retrievals (Holben et al., 1998), to adjust the calibration factor. The AERONET climatology is built using available Direct Sun version 3 level 2.0 hourly retrievals from 2000 to 2014. Events dominated by coarse particles are identified by tagging those scenes where the Angstrom exponent (AE) is lower than 0.75. The monthly means of the climatology are built considering that at least 15 points per month must be available, the averages consider that those events where measurements show AE larger than 0.75 are mostly dominated by fine particles, hence the optical depth of dust in these events is considered zero. The framework for this calibration has been tested with the OpenIFS 48r1 AER dust scheme (Remy et al., 2022, see Figures 1 and 2). Our testbed consisted of a 1-year long experiment considering exclusively natural aerosols. This preliminary comparison suggests that the long-range transport of dust over the Atlantic, as well as the strength of Asian sources may be underestimated. Both aspects will be further investigated with a more thorough evaluation in Task 3.4, including also the anthropogenic component in the model simulations, which was excluded from this first assessment.

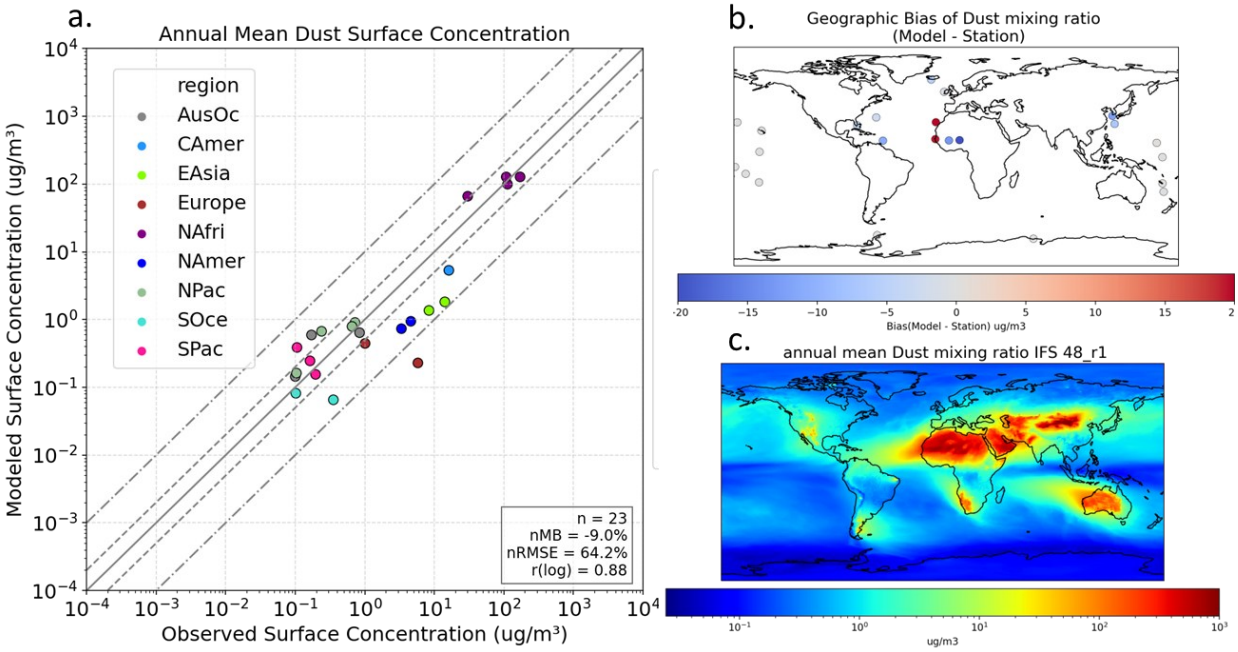

Figure 1. Comparison of (a) the modelled annual mean dust surface concentration (μg/m^3) against climatological mean values from RSMAS sites and AMMA campaign. The solid line represents the 1:1 correspondence, the long-dashed lines show the 10:1 and 1:10 relationships, and the short-dashed lines correspond to a factor of 2, respectively. Colours indicate measurement locations listed in the figure legend. n: number of sites, nMB: normalized mean bias (%), nRMSE: normalized Root Mean Square Error (%). Geographical distribution of the bias (b) between simulated and observed values. (c) Annual mean concentration of simulated dust concentration.

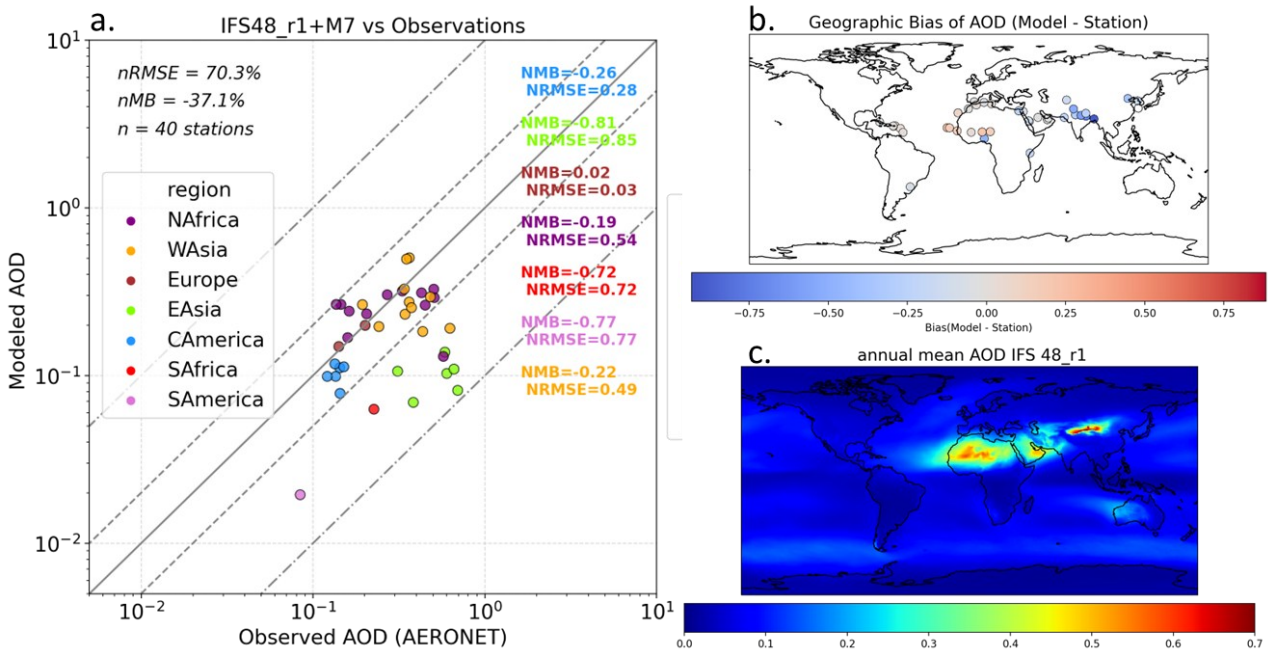

Figure 2. Comparison of (a) the modelled annual mean AOD against climatological mean values from AERONET. The solid line represents the 1:1 correspondence, the long-dashed lines show the 10:1 and 1:10 relationships, and the short-dashed lines correspond to a factor of 2, respectively. Colours indicate measurement locations listed in the figure legend. n: number of sites, nMB: normalized mean bias (%), nRMSE: normalized Root Mean Square Error (%). Geographical distribution of the bias (b) between simulated and observed values. (c) Annual mean concentration of simulated AOD.

This kind of comparison allows to identify the overall performance of the model, and whether regional biases arise. Adjusting regional differences with a global constant scaling factor for dust emission is complicated, but the combined evaluation against DOD and surface concentration also informs us about the balance between dust emission strength and size distribution in the model (i.e., the ratio of coarse to fine dust particles). Furthermore, the Tegen et al. (2002, 2004) allows for a soil-type dependent calibration of the threshold wind friction velocity for dust emission, particularly over cultivated areas, which can also be adjusted based on the observational evidence. The calibration of the Tegen et al. (2002, 2004) dust scheme is ongoing in OpenIFS 48r1 and the final model configuration will be reported under Deliverable 3.4 of FOCI, together with a detailed evaluation against observations.

The second step towards the integration of the mineral dust sensitive ICNC parameterization is the implementation of the quartz and feldspar tracers in the accumulation and coarse modes used for transporting dust in OpenIFS. This is done in an analogous way as the iron oxides introduced to improve the definition of the dust optical properties (see deliverable D3.2). First, the soil mineralogical atlas of Claquin et al. 1999, Nickovic et al. (2012) is used to identify the abundance of quartz and feldspar in the clay (up to 2 μm) and silt (2-63 μm) soil sizes. Then, an extension of the brittle fragmentation theory applied to dust emission (Kok et al., 2011) is used to estimate the mass fraction of the target minerals in the accumulation and coarse modes of the model (Figure 3). These mass fractions can then be applied to the bulk dust emission flux estimated by the model to derive the specific emissions of quartz and feldspar. It must be noted that the amount of K-feldspar, the relevant mineral for ice nucleation, is not provided directly by the soil map, therefore it is assumed to be a constant fraction of the total feldspar (35%, as in Chatziparaschos et al., 2023).

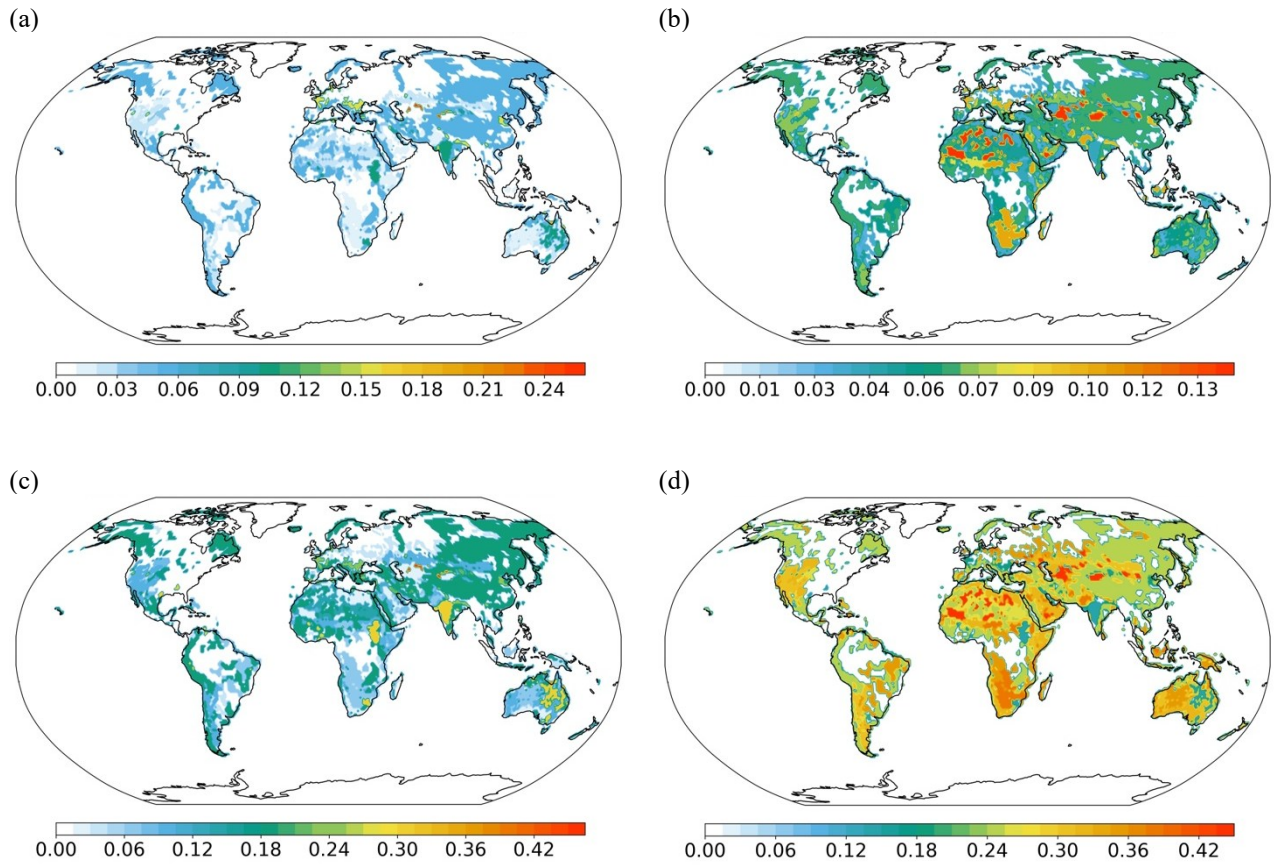

Figure 3. Estimated mass fraction at emission in the EC-Earth4 accumulation (top) and coarse (bottom) modes for feldspar (left) and quartz (right), as derived from the Claquin et al. (1999), with the updates from Nickovic et al. (2012).

Then, the calculation of the ice nucleating particles has to be conducted online. The implementation follows the singular approximation based on the laboratory-derived active site density parameterizations for K-feldspar (for temperatures between -2.5 and -37.5ºC) and quartz (for temperatures between -10.5 and -37.5ºC) provided in Harrison et al. (2019). The mineral particles for this calculation are assumed to be spherical and externally mixed (Atkinson et al., 2013).

In parallel to the technical implementation, a framework for the evaluation of the new cloud scheme has been put in place with a two-fold objective: (1) to verify the new primary ice nucleation scheme, (2) to compare it to the previously existing parameterization for mixed phase clouds.

The evaluation of cloud-related variables in OpenIFS 48r1 is done against satellite observations from MODIS and CALIPSO. To provide context and a basis for comparison, selected results from EC-Earth3-AerChem simulations, featuring both the temperature-based Meyers et al. (1992) and aerosol-sensitive ice nucleation parameterizations developed in previous projects (e.g., FORCeS), are included. These comparisons are intended to help anticipate the behaviour of cloud processes in the EC-Earth4 version, which will be fully described in deliverable D3.4.

The evaluation focuses on total cloud cover (TCC), liquid water path (LWP), ice water path (IWP), and Low-, Mid-, and High-level Cloud Cover (LCC, MCC, and HCC, respectively). The EC-Earth3-AerChem simulations include a baseline configuration using the Meyers parameterization and an aerosol-sensitive version that follows the approaches of Harrison et al. (2019) for immersion freezing of K-feldspar and quartz, Wilson et al. (2015) for marine organic aerosols, and the secondary ice process scheme RaFSIPv2 by Georgakaki and Nenes (2024). For OpenIFS 48r1, two configurations are used, one including the initial implementation of the aerosol module

M7 (baseline, from now on), and the other also incorporating the Morales and Nenes (2014) cloud droplet activation scheme described in section 2.1.1 (MN, from now on). It is worth noting that LCC, MCC, and HCC are directly available as output variables in OpenIFS, while in EC-Earth3-AerChem, these variables were derived using COSP simulator diagnostics.

To establish a consistent reference point, we performed a set of one-year simulations with OpenIFS 48r1 from 1 July 2023 to 30 June 2024. These simulations serve as a solid baseline to evaluate the impacts of upcoming modifications to cloud microphysics in OpenIFS 48r1/EC-Earth4, including aerosol-sensitive parameterizations. In Figure 4, the black line represents the MODIS and CALIPSO observational climatology from 2018, which is used as the reference dataset. The figure also includes EC-Earth3-AerChem simulations in pink (Meyers et al., 1992) and blue (aerosol-sensitive), along with the two OpenIFS 48r1 versions (the baseline in purple and the MN in orange).

The comparison between model simulations and observations reveals several noteworthy patterns. TCC in OpenIFS is reduced in the Northern Hemisphere mid-latitudes compared to both MODIS and EC-Earth3-AerChem, with a localized increase between 20°N and 30°N. LWP is substantially lower in OpenIFS than in EC-Earth3-AerChem within the ±30° latitude band, but it increases at higher latitudes, leading to improved agreement with MODIS observations. In contrast, the IWP is significantly reduced across all latitudes in OpenIFS compared to EC-Earth3-AerChem, resulting in a greater departure from MODIS observations.

LCC in OpenIFS is generally higher than in EC-Earth3-AreChem across most latitudes. Between 40°S and 30°N, this increase brings the simulated LCC closer to CALIPSO observations. MCC is also higher in OpenIFS compared to EC-Earth3-AerChem. At low latitudes, this increase leads to better agreement with observations, but biases grow at higher latitudes. HCC in OpenIFS exhibits mixed behaviour: it is increased at high latitudes, reduced at mid-latitudes, and increased again at low latitudes. Overall, HCC in OpenIFS deviates more from CALIPSO observations than EC-Earth3-AerChem does.

A preliminary evaluation of the changes between the baseline OpenIFS 48r1 M7 and the MN updated simulation, reflects important changes in cloud properties. These include a notable reduction in total cloud cover over the Southern Hemisphere, decreased LWP in the Southern Hemisphere and tropical regions, and reduced IWP in both hemispheres. Additionally, reductions in LCC and MCC are observed in the same regions where LWP decreases, while HCC reductions are concentrated in low and mid-latitudes of the Northern Hemisphere. While these changes are broadly consistent with the expected behaviour of the Morales and Nenes activation scheme.

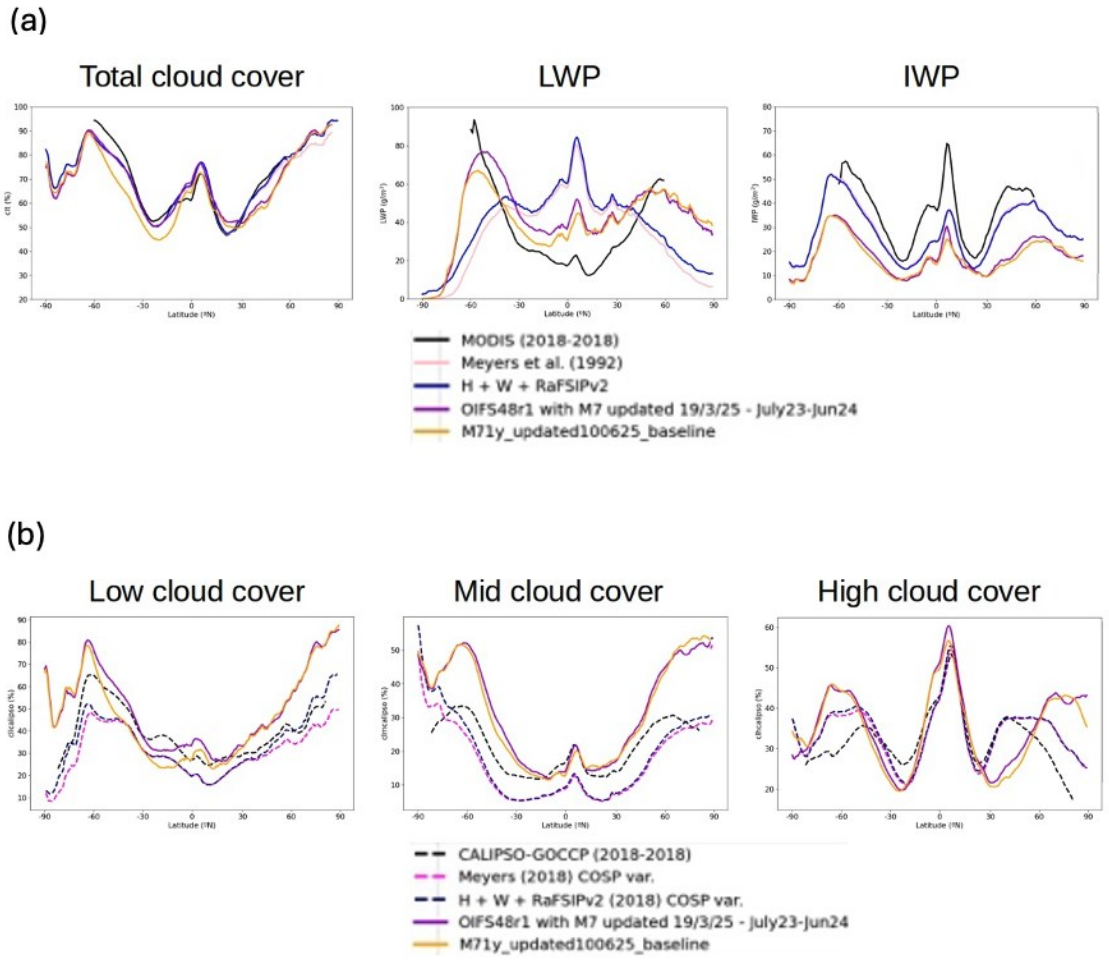

Figure 4. (a) Annual mean total cloud cover (TCC) -%-, liquid water path (LWP) -g/m^2-, ice water path (IWP) -g/m2- as derived from MODIS (black line) and (b) Low, Mid and High Cloud Cover (LCC, MCC, and HCC, respectively) -%- from CALIPSO (black line) compared to EC-Earth3-AerChem with Meyers (pink), aerosol-sensitive parameterization (blue), OpenIFS 48r1 - baseline (purple) and OpenIFS 48r1 - MN (orange), from left to right and top to bottom.

2.2 EMAC

The Modular Earth Submodel System (MESSy), introduced by Jöckel et al. in 2005, serves as a flexible framework for building detailed Earth System Models (ESMs) by utilizing a collection of process-based modules, called submodels. It is structured to allow seamless integration of various model components, featuring standardized interfaces, a consistent coding structure, and a range of submodels developed within this framework. The MESSy architecture is organized into four primary layers: (i) the **Basemodel Layer (BML)**, which typically includes a general circulation model (GCM) or a box model and manages the central clock and run-time controls; (ii) the **Basemodel Interface Layer (BMIL)**, which acts as a communication bridge between the basemodel and the submodels, incorporating MESSy's infrastructure within the basemodel; (iii) the **Submodel Interface Layer (SMIL)**, which facilitates the connection between specific processes and the BMIL infrastructure; and (iv) the **Submodel Core Layer (SMCL)**, which holds the Earth system process implementations or diagnostic tools, independent of the basemodel. The SMCL relies on data from the SMIL and provides data back to the basemodel or other submodels. A detailed list of available submodels in MESSy can be accessed at www.messy-interface.org. Due to ongoing advancements in chemistry-based submodels, MESSy has become a valuable tool for building Chemistry-Climate Models (CCMs). CCMs are sophisticated computational models used to study the complex interactions between atmospheric chemistry and climate variables. They are crucial for isolating specific climate processes and simulating potential future climate scenarios, helping researchers understand how the climate system responds to rapid changes. This in turn aids the development of adaptive strategies and mitigation plans. One of the most common applications of MESSy in CCMs is through its integration with the European Centre for Medium-Range Weather Forecasts – Hamburg v5 (ECHAM5) basemodel, known as EMAC (ECHAM5/MESSy for Atmospheric Chemistry). EMAC was one of the first community-driven models to simulate the interactions between stratospheric and tropospheric chemistry and dynamics in a unified framework within global models (Jöckel et al., 2006).

The aerosol microphysics and the partitioning between gases and aerosols are modeled using the Global Modal-aerosol eXtension (GMXe) aerosol module, as outlined by Pringle et al. (2010). GMXe simulates aerosol distribution across interacting lognormal modes, like the approach used by Vignati et al. (2004). These modes are categorized into four size ranges: nucleation (<6 nm radius), Aitken (6–60 nm), accumulation (60–600 nm), and coarse (>700 nm). Each size category is further divided into hydrophilic (4 modes) and hydrophobic (3 modes) groups. The GMXe model has been thoroughly validated in previous studies (Pozzer et al., 2012).

The CLOUD submodel was originally developed to contain the original cloud microphysics routine from the ECHAM5 from MPI Hamburg. These routines have been modularised and adapted into the MESSy - structure but still perform the same microphysical calculations as the original routine. Further, two-moment cloud microphysics routines developed at the ETH Zürich (Lohmann et al., 2007, 2010) has been implemented so to include detailed microphysics and allowing the implementation of aerosol activation scheme. The standard aerosols activation scheme used by default in EMAC is based on the Abdul-Razzak and Ghan (2000) scheme, combined with the κ-Köhler method (Petters and Kreidenweis, 2007). In addition to the EMAC standard aerosol activation method, two additional activation parametrizations have been included, i.e. the one from Barahona and Nenes (2009), specifically developed for ice and mixed phase clouds and the one of Morales Betancourt and Nenes (2014), specifically developed for warm clouds. Here we report the development of these two parametrizations.

2.2.1 Activation scheme for warm clouds

The formation of cloud droplets is parameterized using the "unified activation framework" (UAF; Kumar et al., 2011; Karydis et al., 2011), a sophisticated, physics-based approach that calculates the equilibrium supersaturation (s) over the surface of a water droplet containing a solute particle. This framework integrates two key theories: the κ-Köhler theory (KT; Petters and Kreidenweis, 2007), which describes the activation of soluble aerosols based on their hygroscopicity parameter (k), and the Frenkel–Halsey–Hill adsorption activation theory (FHH-AT; Kumar et al., 2009), which accounts for droplet activation caused by water adsorption onto insoluble aerosols, such as mineral dust. To determine the amount of aerosol activated based on equilibrium supersaturation, it is necessary to estimate the maximum supersaturation within the rising parcel (model box). The method by Barahona and Nenes (2007) is used for this estimation, where the maximum saturation is influenced by the updraft velocity and the condensational integral, which accounts for the reduction of supersaturation as droplets grow in the updraft. We assume that the in-cloud updraft velocity is proportional to the large-scale updraft velocity in the general circulation model (GCM), excluding convection, and the square root of the turbulent kinetic energy (TKE), assuming that vertical velocity variability is dominated by turbulent transports (proportional to TKE). This approximation has been found to be effective for representing large-scale cloud types, such as stratocumulus, which are modeled in the CLOUD submodel of EMAC. Lastly, the condensational integral is calculated by summing the contributions from particles that adhere to the Köhler theory, using the revised population splitting method of Morales Betancourt and Nenes (2014). It also incorporates contributions from both freshly emitted and aged dust particles, as described by Kumar et al. (2009) and Karydis et al. (2011).

We evaluated the model implementation using the standard configuration in EMAC, utilizing the GMXe aerosols submodel to represent the aerosol spectral distribution. Aerosol modes composed solely of soluble material and following the Köhler theory (KT) require the calculation of effective hygroscopicity (κ), which is derived from the chemical composition of the aerosol mode using the ISORROPIA thermodynamic equilibrium model (Fountoukis and Nenes, 2007). The predicted in-cloud cloud droplet number concentration (CDNC) is compared with observational data from diverse regions, including continental, polluted marine, and clean marine areas worldwide. To align the model results with the observations, the locations (longitude, latitude, altitude) and seasonal timing of the observations were considered. We implicitly assume that inter-annual variability is negligible, and thus, only a single year of simulation is performed. It's important to note that the observational data typically represent point measurements, not monthly averages over 1.9° grid squares as sampled in the model, making this comparison more qualitative than quantitative.

A summary of the comparison's results is shown in Figure 5. Overall, the model shows a good agreement with the observational dataset from 75 locations, yielding a mean bias of 132 cm-3, a normalized mean bias of 82%, and a normalized mean error of 56%. Notably, the model's improved performance indicates larger CDNC in continental regions compared to clean marine regions, consistent with observational data.

Figure 6 shows the annual mean cloud droplet number concentration (CDNC) calculated by EMAC using the UAF implementation for the lowest model level where cloud formation occurs (centred at 940 hPa). Here, CDNC refers to the number concentration of droplets that are nucleated within the cloud, providing an upper bound since processes like droplet depletion due to collision, coalescence, and collection are not included. The predicted annual mean CDNC over continental regions is 546 cm^{-3}, with values exceeding 1000 cm^{-3} in industrialized areas such as Europe, central and eastern Asia, and North America. These regions exhibit high aerosol number concentrations, exceeding 10,000 cm^{-3}, while the calculated updraft velocities (ranging from 0.5 to 1 m/s) lead to maximum supersaturations (0.1–0.3%) that are sufficient to activate between 5% (over eastern China) and 15% (over central Europe) of the pollution aerosols into cloud droplets.

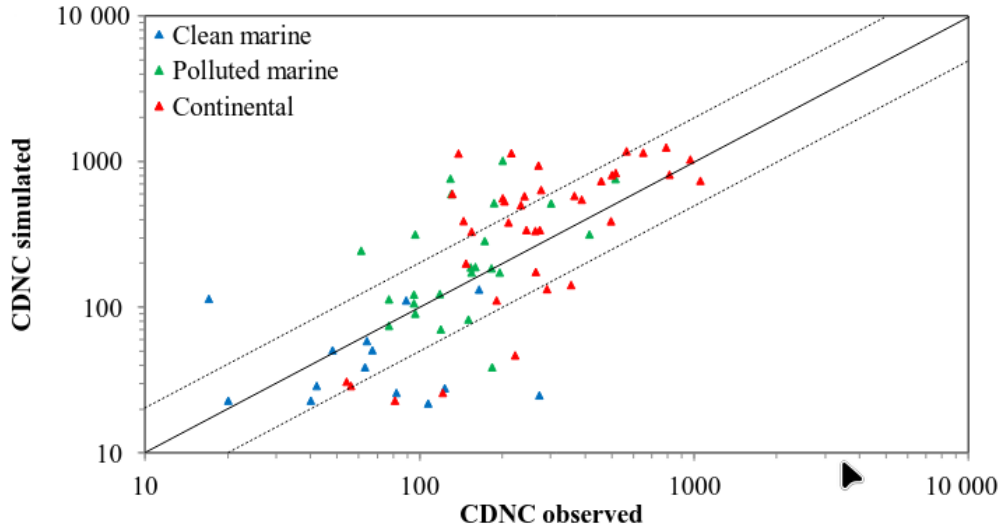

Figure 5. Scatterplot comparing model simulated cloud droplet number concentrations (cm−3) against 75 observational datasets worldwide, derived from in situ measurements and satellite retrievals, also shown are the 1:1, 2:1 and 1:2 lines. Adapted from Karydis et al. (2017)

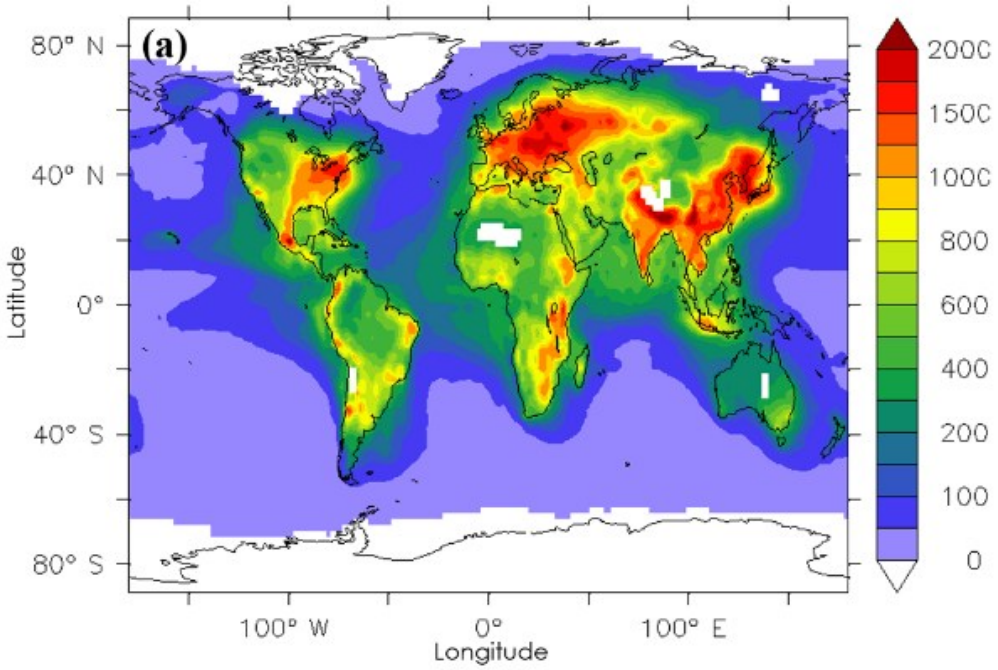

Figure 6. Predicted in-cloud annual mean cloud droplet number concentrations (cm−3) at the lowest cloud-forming. Adopted from Karydis et al.(2017)

2.2.2 Activation scheme for ice and mixed phase clouds

Ice crystal formation occurs via both homogeneous and heterogeneous nucleation, depending on environmental factors such as temperature, supersaturation, vertical velocity, and aerosol characteristics (e.g., number concentration and physicochemical properties). Homogeneous nucleation happens when supercooled liquid droplets freeze at low temperatures ($T < 238$ K) and high ice supersaturation (140%–160%) (Koop et al., 2000).

In contrast, heterogeneous nucleation occurs when ice forms on the surface of an aerosol particle, lowering the energy barrier for ice nucleation. This allows ice crystals to form at lower supersaturations and/or at higher subfreezing temperatures compared to homogeneous nucleation. The particles responsible for ice crystal formation are called ice nucleating particles (INPs), which are primarily insoluble materials like mineral dust, soot, organics, and biological particles.

There are two main regimes for ice crystal formation: the cirrus regime, which occurs at low temperatures ($T < 238$ K) and involves both homogeneous and heterogeneous nucleation, and the mixed-phase regime, which occurs at subfreezing temperatures (between 238 and 273 K) where ice crystals form solely through heterogeneous nucleation. Since heterogeneous nucleation occurs at lower supersaturations than homogeneous nucleation, the available water vapor decreases, reducing or preventing homogeneous nucleation. The competition between these two processes can significantly influence ice crystal number concentrations (ICNCs) in the cirrus regime, even when INP concentrations are low. Therefore, accurately parameterizing nucleation processes is critical for representing ice formation in atmospheric models.

The Barahona and Nenes (2009) parameterization offers a computationally efficient way to model ice nucleation and is well-suited for large-scale atmospheric models. It explicitly accounts for the competition for water vapor between homogeneous and heterogeneous nucleation in the cirrus regime, the effect of chemically heterogeneous and polydisperse aerosols acting as INPs, and allows flexibility in using different heterogeneous nucleation parameterizations. We implemented the ICNC calculation scheme of Barahona and Nenes (2009) in EMAC, following the approach outlined by Bacer et al. (2018).

Figure 7 presents the spatial distribution of ICNC burdens during winter (DJF) and summer (JJA) for both a 10-year climatology of DARDAR-Nice retrievals and the results from our model simulation. The satellite data show high ICNC values primarily in deep convective regions and mid-latitudes during the winter months, likely due to higher ice nucleation rates associated with strong wind velocities. These patterns are broadly reflected in the model's ICNC burden distribution, which agrees well with the satellite data overall. However, the absolute values differ by approximately an order of magnitude, with ICNC burdens of up to 10^9 m^{-2} in DARDAR-Nice and 10^{10} m^{-2} in EMAC in these regions. A larger discrepancy is observed over Antarctica, where the model overestimates ICNCs, likely due to persistently low temperatures (below −35°C) and high supersaturation levels. In mountainous regions, the model simulates even higher ICNC values, up to 10^{11} m^{-2}. Similar ICNC magnitudes have been reported in other modelling studies (e.g., Bacer et al., 2018). Although increases in ICNC around steep orographic features are visible in the satellite data, they primarily occur at temperatures between the homogeneous nucleation threshold and −60°C, where ICNCs locally reach up to 300 L^{-1}—nearly three times higher than surrounding values.

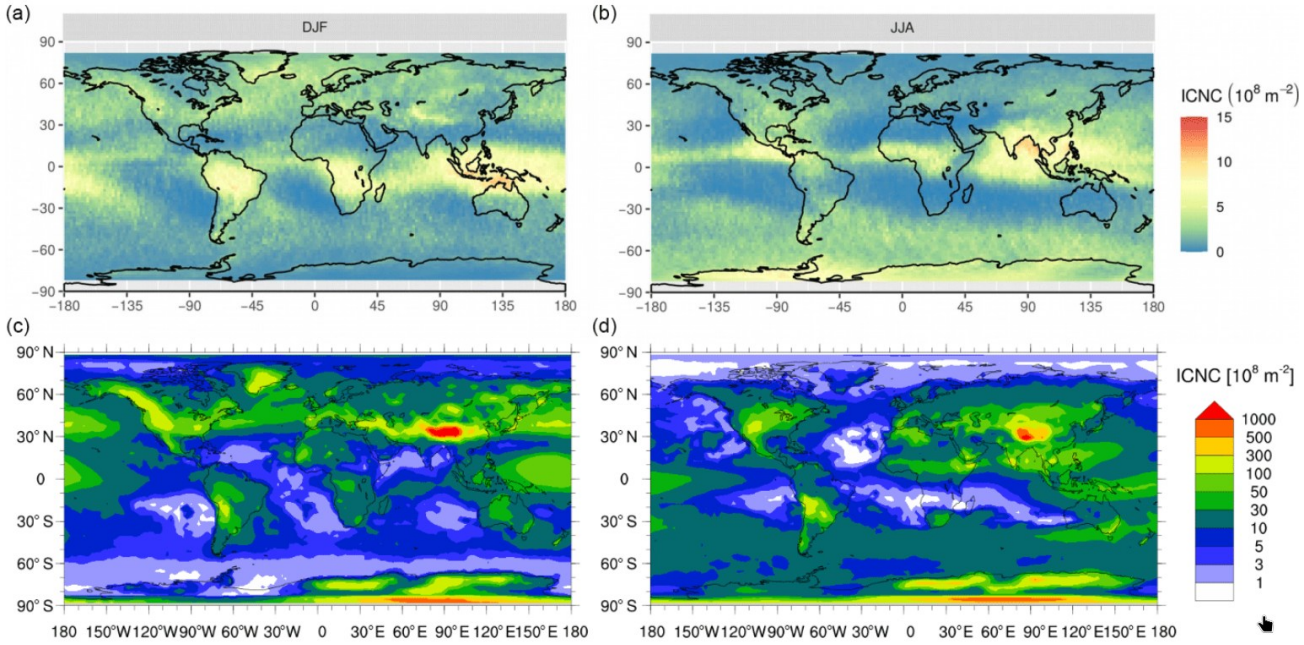

Figure 7. Mean spatial distribution of vertically integrated ICNC burden for the DJF and JJA seasons. **(a, b)** In-cloud ICNC burden retrieved by DARDAR-Nice (2006–2017) averaged in a grid. **(c, d)** In-cloud ICNC burden computed by EMAC (REF 5 h output greater than zero were considered in the average). Adapted from Bacer et al. (2021)

3. OUTLOOK

This report presents the developments introduced in the representation of aerosol-cloud interactions in the two ESMs involved in the FOCI project, EC-Earth4 and EMAC. For EC-Earth, aerosol activation was originally absent in IFS and OpenIFS but has now been implemented in OpenIFS 48r1 by porting the EC-Earth3 activation scheme based on Abdul-Razzak and Ghan (2000) and complemented with the Morales Betancourt and Nenes (2014) activation parameterization with refinements in the updraft velocity calculations. Within FOCI, we contributed by testing the new activation code, integrating it with other aerosol-chemistry developments described in Deliverable D3.1, and extending the framework to include dust-cloud interactions. Specifically, a new dust emission module based on Tegen et al. (2002, 2004) was introduced, enabling the calculation of mineral mass fractions of quartz and K-feldspar at emission and their role as efficient ice nucleating particles, thereby linking to the ice crystal number concentration (ICNC) in OpenIFS 48r1. In EMAC, the standard Abdul-Razzak and Ghan (2000) activation scheme has been complemented with two additional parameterizations: Barahona and Nenes (2009), designed for ice and mixed-phase clouds, and Morales Betancourt and Nenes (2014), tailored for warm clouds.

Initial evaluations of these new implementations have been carried out during the development phase and reported here. More extensive assessments against broader observational datasets are planned within Task 3.4 of WP3 and will be reported in Deliverable D3.4. This report documents the new aerosol-cloud interaction developments and closes the series of three reports providing details on the advancements made within FOCI project in the representation of aerosols and chemistry (Deliverable D3.1), aerosol-radiation interaction (Deliverable D3.2), and aerosol-cloud interaction (Deliverable D3.3).

REFERENCES

Abdul-Razzak, H. and Ghan, S. J.: A parameterization of aerosol activation: 2. Multiple aerosol types, J. Geophys. Res., 105, 6837–6844, https://doi.org/10.1029/1999JD901161, 2000.

Albani, S., Mahowald, N. M., Perry, A., Scanza, R. A., Zender, C. S., Heavens, N., Maggi, V., Kok, J. F., and Otto-Bliesner, B.: Improved dust representation in the Community Atmosphere Model, J. Adv. Model. Earth Sy., 6, 541–570, https://doi.org/10.1002/2013MS000279, 2014.

Arimoto, R., Duce, R. A., Ray, B. J., Ellis, W. G., Cullen, J. D., and Merrill, J. T.: Trace elements in the atmosphere over the North Atlantic, J. Geophys. Res., 100, 1199–1213, https://doi.org/10.1029/94JD02618, 1995.

Atkinson, J. D., Murray, B. J., Woodhouse, M. T., Whale, T. F., Baustian, K. J., Carslaw, K. S., Dobbie, S., O'Sullivan, D., and Malkin, T. L.: The importance of feldspar for ice nucleation by mineral dust in mixed-phase clouds, Nature, 498, 355–358, https://doi.org/10.1038/nature12278, 2013.

Barahona, D., Breen, K. H., Kalesse-Los, H., and Röttenbacher, J.: Deep learning parameterization of vertical wind velocity variability via constrained adversarial training, Artif. Intell. Earth Syst., 3, e230025, https://doi.org/10.1175/AIES-D-23-0025.1, 2023.

Barahona, D. and Nenes, A.: Parameterization of cloud droplet formation in large-scale models: Including effects of entrainment, J. Geophys. Res., 112, D16206, doi:10.1029/2007JD008473, 2007.

Barahona, D. and Nenes, A.: Parameterization of cirrus cloud formation in large-scale models: Homogeneous nucleation, J. Geophys. Res.-Atmos., 113, d11211, https://doi.org/10.1029/2007JD009355, 2008

Barahona, D. and Nenes, A.: Parameterizing the competition between homogeneous and heterogeneous freezing in ice cloud formation – polydisperse ice nuclei, Atmos. Chem. Phys., 9, 5933–5948, https://doi.org/10.5194/acp-9-5933-2009, 2009

Chang, D.Y., Lelieveld, J., Tost, H., Steil, B., Pozzer, A. and Yoon, J., 2017. Aerosol physicochemical effects on CCN activation simulated with the chemistry-climate model EMAC. Atmospheric Environment, 162, pp.127-140.

Chatziparaschos, M., Daskalakis, N., Myriokefalitakis, S., Kalivitis, N., Nenes, A., Gonçalves Ageitos, M., Costa-Surós, M., Pérez García-Pando, C., Zanoli, M., Vrekoussis, M., and Kanakidou, M.: Role of K-feldspar and quartz in global ice nucleation by mineral dust in mixed-phase clouds, Atmos. Chem. Phys., 23, 1785–1801, https://doi.org/10.5194/acp-23-1785-2023, 2023.

Claquin, T., Schulz, M., and Balkanski, Y. J.: Modeling the mineralogy of atmospheric dust sources, J. Geophys. Res.-Atmos., 104, 22243–22256, https://doi.org/10.1029/1999JD900416, 1999

Fountoukis, C. and Nenes, A.: ISORROPIA II: a computationally efficient thermodynamic equilibrium model for K+–Ca2+– Mg2+—Na+——Cl−–H2O aerosols, Atmos. Chem. Phys., 7, 4639–4659, https://doi.org/10.5194/acp-7-4639-2007, 2007.

Georgakaki, P., & Nenes, A. (2024). RaFSIP: Parameterizing ice multiplication in models using a machine learning approach. *Journal of Advances in Modeling Earth Systems*, 16, e2023MS003923. https://doi.org/10.1029/2023MS003923

Gkikas, A., Proestakis, E., Amiridis, V., Kazadzis, S., Di Tomaso, E., Tsekeri, A., Marinou, E., Hatzianastassiou, N., and Pérez García-Pando, C.: ModIs Dust AeroSol (MIDAS): a global fine-resolution dust optical depth data set, Atmos. Meas. Tech., 14, 309–334, https://doi.org/10.5194/amt-14-309-2021, 2021.

Gkikas, A., Proestakis, E., Amiridis, V., Kazadzis, S., Di Tomaso, E., Marinou, E., Hatzianastassiou, N., Kok, J. F., and García-Pando, C. P.: Quantification of the dust optical depth across spatiotemporal scales with the MIDAS global dataset (2003–2017), Atmos. Chem. Phys., 22, 3553–3578, https://doi.org/10.5194/acp-22-3553-2022, 2022.

Harrison, A. D., Lever, K., Sanchez-Marroquin, A., Holden, M. A., Whale, T. F., Tarn, M. D., McQuaid, J. B., and Murray, B. J.: The ice-nucleating ability of quartz immersed in water and its atmospheric importance

compared to K-feldspar, Atmos. Chem. Phys., 19, 11343–11361, https://doi.org/10.5194/acp-19-11343-2019, 2019

Holben, B. N., Eck, T. F., Slutsker, I., Tanré, D., Buis, J. P., Setzer, A., Vermote, E., Reagan, J. A., Kaufman, Y. J., Nakajima, T., Lavenu, F., Jankowiak, I., and Smirnov, A.: AERONET – A federated instrument network and data archive for aerosol characterization, Remote Sens. Environ., 66, 1–16, https://doi.org/10.1016/S0034-4257(98)00031-5, 1998.

Jöckel, P., Sander, R., Kerkweg, A., Tost, H., & Lelieveld, J.: Technical Note: The Modular Earth Submodel System (MESSy) – a new approach towards Earth System Modeling, Atmospheric Chemistry and Physics, 5, 433–444, https://doi.org/10.5194/acp-5-433-2005, 2005.

Jöckel, P., Tost, H., Pozzer, A., Brühl, C., Buchholz, J., Ganzeveld, L., Hoor, P., Kerkweg, A., Lawrence, M. G., Sander, R., Steil, B., Stiller, G., Tanarhte, M., Taraborrelli, D., van Aardenne, J., & Lelieveld, J.: The atmospheric chemistry general circulation model ECHAM5/MESSy1: consistent simulation of ozone from the surface to the mesosphere, Atmospheric Chemistry and Physics, 6, 5067–5104, https://doi.org/10.5194/acp-6-5067-2006, 2006.

Karydis, V. A., Kumar, P., Barahona, D., Sokolik, I. N., and Nenes, A.: On the effect of dust particles on global cloud condensation nuclei and cloud droplet number, J. Geophys. Res.-Atmos., 116, D23204, https://doi.org/10.1029/2011JD016283, 2011

Karydis, V. A., Tsimpidi, A. P., Bacer, S., Pozzer, A., Nenes, A., and Lelieveld, J.: Global impact of mineral dust on cloud droplet number concentration, Atmos. Chem. Phys., 17, 5601–5621, https://doi.org/10.5194/acp-17-5601-2017, 2017.

Kok, J. F.: A scaling theory for the size distribution of emitted dust aerosols suggests climate models underestimate the size of the global dust cycle, P. Natl. Sci. USA, 108, 1016–1021, https://doi.org/10.1073/pnas.1014798108, 2011.

Koop, T., Luo, B., Tsias, A., and Peter, T.: Water activity as the determinant for homogeneous ice nucleation in aqueous solutions, Nature, 406, 611–614, https://doi.org/10.1038/35020537, 2000.

Kumar, P., Sokolik, I. N., and Nenes, A.: Cloud condensation nuclei activity and droplet activation kinetics of wet processed regional dust samples and minerals, Atmos. Chem. Phys., 11, 8661–8676, https://doi.org/10.5194/acp-11-8661-2011, 2011.

Kumar, P., Sokolik, I. N., and Nenes, A.: Parameterization of cloud droplet formation for global and regional models: including adsorption activation from insoluble CCN, Atmos. Chem. Phys., 9, 2517–2532, https://doi.org/10.5194/acp-9-2517-2009, 2009.

Lohmann, U., Stier, P., Hoose, C., Ferrachat, S., Kloster, S., Roeckner, E., and Zhang, J.: Cloud microphysics and aerosol indirect effects in the global climate model ECHAM5-HAM, Atmos. Chem. Phys., 7, 3425–3446, https://doi.org/10.5194/acp-7-3425-2007, 2007

Lohmann, U. and Ferrachat, S.: Impact of parametric uncertainties on the present-day climate and on the anthropogenic aerosol effect, Atmos. Chem. Phys., 10, 11373–11383, doi:10.5194/acp-10-11373-2010, 2010

Marticorena, B., Chatenet, B., Rajot, J. L., Traoré, S., Coulibaly, M., Diallo, A., Koné, I., Maman, A., NDiaye, T., and Zakou, A.: Temporal variability of mineral dust concentrations over West Africa: analyses of a pluriannual monitoring from the AMMA Sahelian Dust Transect, Atmos. Chem. Phys., 10, 8899–8915, https://doi.org/10.5194/acp-10-8899-2010, 2010.

Meyers, M. P., DeMott, P. J., and Cotton, W. R.: New primary icenucleation parameterizations in an explicit cloud model, J. Appl. Meteorol. Climatol., 31, 708–721, https://doi.org/10.1175/1520-0450(1992)031<0708:NPINPI>2.0.CO;2, 1992.

Morales Betancourt, R. and Nenes, A.: Droplet activation parameterization: the population-splitting concept revisited, Geosci. Model Dev., 7, 2345–2357, https://doi.org/10.5194/gmd-7-2345-2014, 2014.

Petters, M. D. and Kreidenweis, S. M.: A single parameter representation of hygroscopic growth and cloud condensation nucleus activity, Atmos. Chem. Phys., 7, 1961–1971, https://doi.org/10.5194/acp-7-1961-2007, 2007.

Pozzer, A., de Meij, A., Pringle, K. J., Tost, H., Doering, U. M., van Aardenne, J., & Lelieveld, J.: Distributions and regional budgets of aerosols and their precursors simulated with the EMAC chemistry-climate model, Atmospheric Chemistry and Physics, 12, 961–987, https://doi.org/10.5194/acp-12-961-2012 , 2012.

Pringle, K. J., Tost, H., Metzger, S., Steil, B., Giannadaki, D., Nenes, A., Fountoukis, C., Stier, P., Vignati, E., & Lelieveld, J.: Description and evaluation of GMXe: a new aerosol submodel for global simulations (v1), Geoscientific Model Development, 3, 391–412, https://doi.org/10.5194/gmd-3-391-2010 , 2010.

Prospero, J. M.: The Atmospheric Transport of Particles to the Ocean, in: Particle Flux in the Ocean, edited by: Ittekkot, V., Schafer, P., Honjo, S., and Depetris, P. J., Wiley, New York, 19–52, ISBN 978-0471960737, 1996.

Prospero, J. M.: Long-term measurements of the transport of African mineral dust to the southeastern United States: Implications for regional air quality, J. Geophys. Res.-Atmos., 104, 15917–15927, https://doi.org/10.1029/1999JD900072, 1999.

Rémy, S., Kipling, Z., Huijnen, V., Flemming, J., Nabat, P., Michou, M., Ades, M., Engelen, R., and Peuch, V.-H.: Description and evaluation of the tropospheric aerosol scheme in the Integrated Forecasting System (IFS-AER, cycle 47R1) of ECMWF, Geosci. Model Dev., 15, 4881–4912, https://doi.org/10.5194/gmd-15-4881-2022, 2022.

Ridley, D. A., Heald, C. L., Kok, J. F., and Zhao, C.: An observationally constrained estimate of global dust aerosol optical depth, Atmos. Chem. Phys., 16, 15097–15117, https://doi.org/10.5194/acp-16-15097-2016, 2016.

Riipinen, I., Talvinen, S., et al.: Treatment of Key Aerosol and Cloud Processes in Earth System Models – Recommendations from the FORCeS Project, Tellus B: Chemical and Physical Meteorology, submitted.

Tegen, I., Harrison, S. P., Kohfeld, K., Prentice, I. C., Coe, M., and Heimann, M.: Impact of vegetation and preferential source areas on global dust aerosol: Results from a model study, J. Geophys. Res., 107(D21), 4576, https://doi.org/10.1029/2001JD000963, 2002.

Tegen, I., Werner, M., Harrison, S. P., and Kohfeld, K. E.: Relative importance of climate and land use in determining present and future global soil dust emission, Geophys. Res. Lett., 31, L05105, https://doi.org/10.1029/2003GL019216, 2004.

Thomas, M. A., Wyser, K., Wang, S., Chatziparaschos, M., Georgakaki, P., Costa-Surós, M., Gonçalves Ageitos, M., Kanakidou, M., García-Pando, C. P., Nenes, A., van Noije, T., Le Sager, P., and Devasthale, A.: Recent improvements and maximum covariance analysis of aerosol and cloud properties in the EC-Earth3-AerChem model, Geosci. Model Dev., 17, 6903–6927, https://doi.org/10.5194/gmd-17-6903-2024, 2024.

van Noije, T., Bergman, T., Le Sager, P., O'Donnell, D., Makkonen, R., Gonçalves-Ageitos, M., Döscher, R., Fladrich, U., von Hardenberg, J., Keskinen, J.-P., Korhonen, H., Laakso, A., Myriokefalitakis, S., Ollinaho, P., Pérez García-Pando, C., Reerink, T., Schrödner, R., Wyser, K., and Yang, S.: EC-Earth3-AerChem: a global climate model with interactive aerosols and atmospheric chemistry participating in CMIP6 , Geosci. Model Dev., 14, 5637–5668, https://doi.org/10.5194/gmd-14-5637-2021, 2021.

Vignati, Elisabetta, Julian Wilson, and Philip Stier. "M7: An efficient size-resolved aerosol microphysics module for large-scale aerosol transport models." Journal of Geophysical Research: Atmospheres 109.D22 (2004).

Voss, K. K., and A. T. Evan, 2020: A New Satellite-Based Global Climatology of Dust Aerosol Optical Depth. *J. Appl. Meteor. Climatol.*, **59**, 83–102, https://doi.org/10.1175/JAMC-D-19-0194.1.

Wilson, T. W., Ladino, L. A., Alpert, P. A., Breckels, M. N., Brooks, I. M., Browse, J., Burrows, S. M., Carslaw, K. S., Huffman, J. A., Judd, C., Kilthau, W. P., Mason, R. H., McFiggans, G., Miller, L. A., Nájera, J. J., Polishchuk, E., Rae, S., Schiller, C. L., Si, M., Temprado, J. V., Whale, T. F., Wong, J. P. S., Wurl, O., Yakobi-Hancock, J. D., Abbatt, J. P. D., Aller, J. Y., Bertram, A. K., Knopf, D. A., and Murray, B. J.: A marine biogenic source of atmospheric ice-nucleating particles, Nature, 525, 234–238, https://doi.org/10.1038/nature14986, 2015.